



Simulation of Geothermal Flow in Deep Sedimentary Basins in Alberta

Simulation of Geothermal Flow in Deep Sedimentary Basins in Alberta

T. Graf

Energy Resources Conservation Board
Alberta Geological Survey

July 2009

©Her Majesty the Queen in Right of Alberta, 2009
ISBN 978-0-7785-6980-0

The Energy Resources Conservation Board/Alberta Geological Survey (ERCB/AGS) and its employees and contractors make no warranty, guarantee or representation, express or implied, or assume any legal liability regarding the correctness, accuracy, completeness or reliability of this publication. Any software supplied with this publication is subject to its licence conditions. Any references to proprietary software in the documentation, and/or any use of proprietary data formats in this release, do not constitute endorsement by ERCB/AGS of any manufacturer's product.

When using information from this publication in other publications or presentations, due acknowledgment should be given to the ERCB/AGS. The following reference format is recommended:

Graf, T. (2009): Simulation of geothermal flow in deep sedimentary basins in Alberta; Energy Resources Conservation Board, ERCB/AGS Open File Report 2009-11, 17 p.

Published July 2009 by:

Energy Resources Conservation Board
Alberta Geological Survey
4th Floor, Twin Atria Building
4999 – 98th Avenue
Edmonton, Alberta
T6B 2X3
Canada

Tel: 780-422-1927

Fax: 780-422-1918

E-mail: AGS-Info@ercb.ca

Website: www.ags.gov.ab.ca

Contents

Acknowledgments.....	v
Abstract.....	vi
1 Introduction.....	1
2 Mathematical Model.....	3
2.1 Model Selection.....	3
2.2 Governing Equations.....	3
2.2.1 Fluid Flow.....	3
2.2.2 Heat Transfer.....	5
2.2.3 Constitutive Equations.....	6
2.2.4 Coupled System.....	6
2.3 Model Development.....	8
2.4 Model Verification.....	9
2.4.1 Elder (1967) Problem.....	9
2.4.2 Caltagirone (1982) Analytical Solution.....	10
3 Geothermal Test Case.....	12
4 Model Applicability and Outlook.....	14
5 References.....	15

Tables

Table 1. Parameters for the Elder (1967) thermal-convection problem (Oldenburg et al., 1995).	10
---	----

Figures

Figure 1. Block model of geological formations that represent a geothermal reservoir.....	1
Figure 2. Cross-sectional view (AA') across the Western Canada Sedimentary Basin in Alberta.....	2
Figure 3. Horizontal distribution of the integral geothermal gradient (between bottom and top of the sedimentary column) in the Western Canada Sedimentary Basin.....	4
Figure 4. Variation of water density and viscosity with temperature.....	7
Figure 5. Picard iteration to solve for variable-density variable-viscosity geothermal flow.....	8
Figure 6. Configuration of the Elder problem.....	9
Figure 7. Verification of the HydroGeoSphere model with the Elder problem of free thermal convection.	10
Figure 8. Conceptual 2-D model for the model verification with the Caltagirone analytical solution.....	12
Figure 9. Verification of the HydroGeoSphere model with the Caltagirone analytical solution.....	13

Acknowledgments

The author's discussions with T. Lemay (Alberta Geological Survey) improved the report and are greatly appreciated. The author acknowledges M. Grobe for carefully reviewing an earlier form of this report.

Abstract

With geothermal gradients of up to 50°C/km, Alberta has the potential to use geothermal energy economically. Mathematical models are excellent tools to predict the flow of geothermal energy and to forecast the productivity of a geothermal reservoir.

This report investigates the flow of geothermal energy under the influence of water-density variations due to temperature changes. As temperature increases, water density decreases, leading to upwelling of hot water. The associated interaction between heat flux and water flow is simulated numerically using an extended version of the HydroGeoSphere model that has been further developed by the author.

The author developed a groundwater model that numerically simulates the coupled flow of formation fluids and geothermal energy. The model accounts for variations of fluid density and viscosity and for buoyancy-induced groundwater flow. A wide temperature range of 0°C to 300°C is covered. The model has been verified against existing numerical and analytical test cases of free, convective, geothermal-groundwater flow. Future work will also incorporate the effect of water salinity on buoyancy-induced fluid flow.

1 Introduction

In geothermal reservoirs, heat is created within the mantle or crust through the decay of radioactive isotopes (Figure 1). Within a sedimentary basin, this heat is transferred to the surface through conduction and convection of fluids. Current geothermal gradients are controlled by the combination of conduction and convection, and can vary due to the relative importance of each.

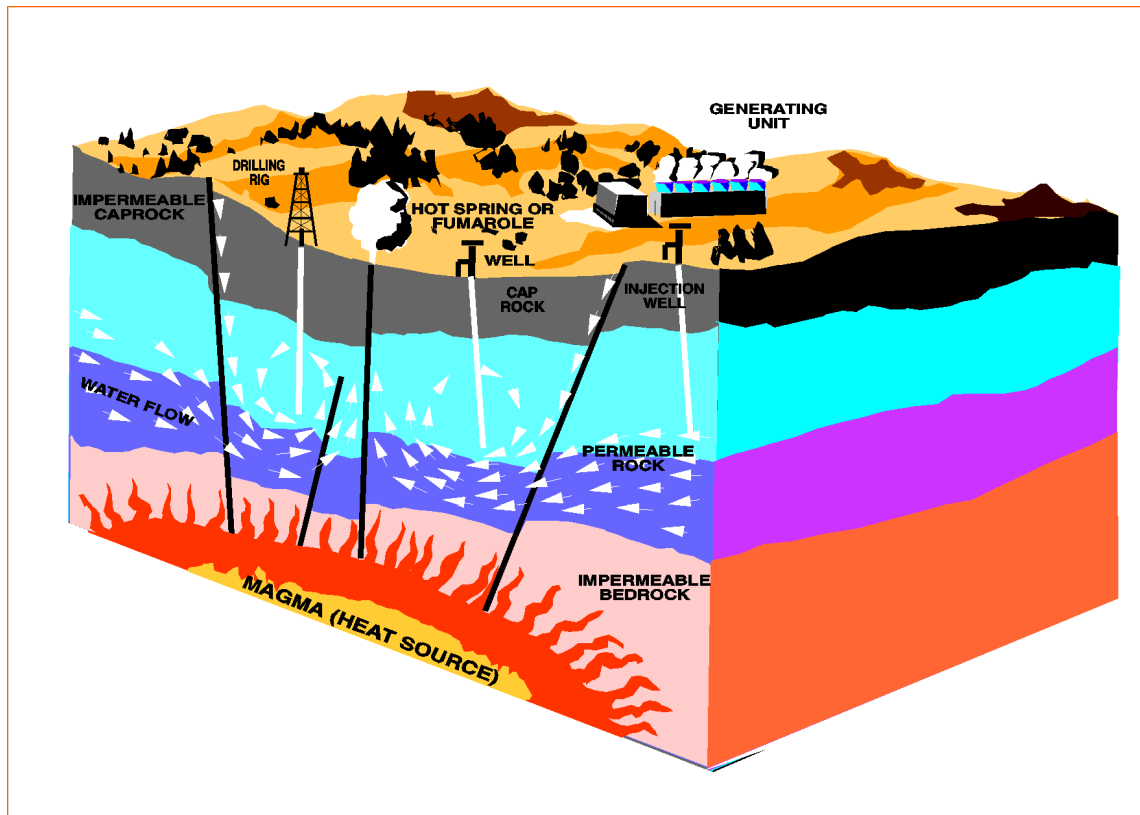


Figure 1. Block model of geological formations that represent a geothermal reservoir (from Energy Information Administration, 1991). The existence of a heat source may induce convective (rotatory) groundwater flow, indicated by white arrowheads. Flowing groundwater transports geothermal energy and therefore controls the efficiency of a geothermal reservoir.

In the Western Canada Sedimentary Basin (situated mainly in Alberta), convective geothermal-energy transport is generally driven by recharge in the foothills and Rocky Mountains, flowing down into the basin and then updip to the northeast and east (Figure 2; Hitchon, 1969). Flowing groundwater takes up the geothermal energy from the Earth's crust and transports part of it in the direction of water flow. Productivity of a geothermal reservoir is controlled predominantly by the geothermal gradient (i.e., temperature variation with depth) encountered in a basin. Clearly, the higher the geothermal gradient, the higher the potential productivity of the geothermal reservoir.

Extremely high gradients (200°C/km) are observed along oceanic spreading centres (e.g., the Mid-Atlantic Rift) and along island arcs (e.g., the Aleutian chain). In Iceland, geothermal energy, the main source of energy, is extracted from areas with geothermal gradients $\geq 40^\circ\text{C}/\text{km}$. Low gradients are observed in tectonic subduction zones because of thrusting of cold, water-filled sediments beneath an existing crust. Tectonically stable shield areas and sedimentary basins have average gradients that typically vary from 15 C/km to 30°C/km.

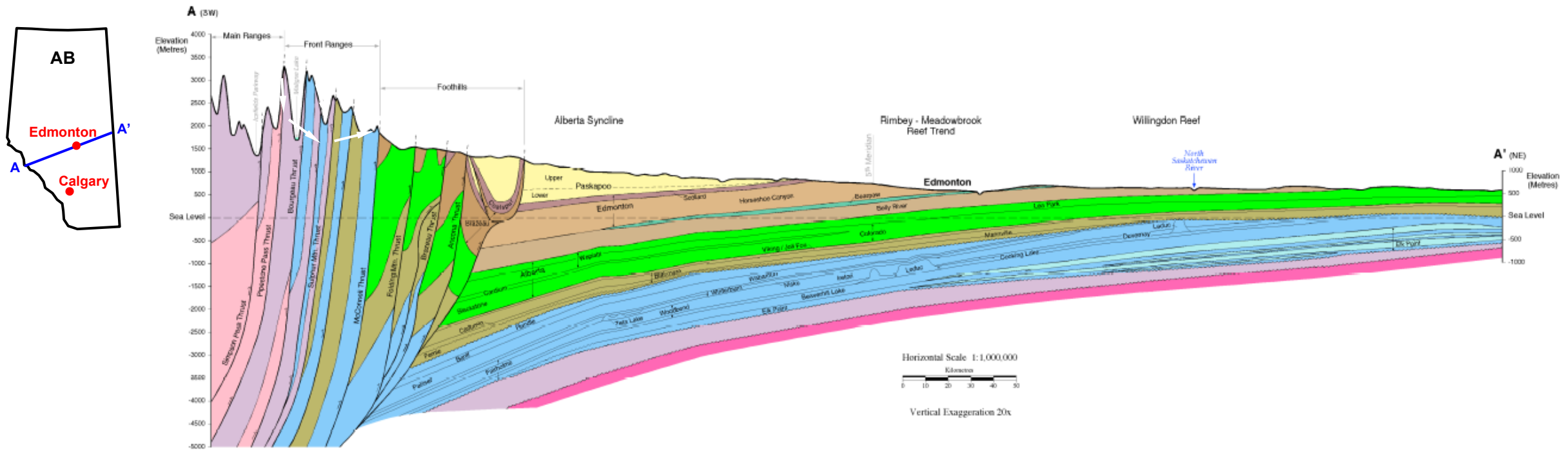


Figure 2. Cross-sectional view (AA') across the Western Canada Sedimentary Basin in Alberta. White arrows indicate the groundwater-flow direction updip the basin from the Rocky Mountains toward northeast.

In Alberta, the average geothermal gradient is about 30°C/km (Majorowicz and Jessop, 1981; Hitchon, 1984). Past studies of the geothermal regime in the Western Canada Sedimentary Basin have shown the existence of a low geothermal gradient of 20°C/km (corresponding to an area of low geothermal-heat flux) in the foothills region of southwestern Alberta, and of a high geothermal gradient of 50°C/km (high geothermal-heat flux) in the lowlands of northeastern Alberta, close to the Precambrian Shield. The horizontal distribution of geothermal gradients and heat fluxes were attributed to the effects of basin-wide groundwater flow in different rock types and are illustrated in Figure 3 (Lam and Jones, 1986; Bachu, 1989; Bachu and Burwash, 1994).

Understanding groundwater flow in a sedimentary basin is crucial to reliably predicting geothermal-energy productivity. In the deeper portion of the Western Canada Sedimentary Basin, variations in water density can control groundwater flow. With the geothermal gradient of 30°C/km and the basin-fill thickness of 4 km, water temperatures could reach 100°C and more. As a consequence of elevated temperature, water density decreases, thereby creating the potentially unstable situation where denser fluid overlies less dense fluid. This situation may lead to upwelling of warm water and to an increase in geothermal productivity.

The objective of this report is to document the development of a groundwater software tool that can be used to forecast density-driven flow of geothermal energy on the sedimentary-basin scale.

2 Mathematical Model

2.1 Model Selection

The HydroGeoSphere model (Therrien et al., 2008) has been selected for this project. HydroGeoSphere is a three-dimensional (3-D) saturated-unsaturated numerical groundwater-flow and multicomponent solute-transport model that has been modified here to solve for coupled variable-density flow and geothermal-energy transport using the fluid-pressure formulation. The porous low-permeability matrix is represented by regular 3-D blocks. Assuming undistorted finite elements allows an analytical discretization of the governing equations by means of elemental-influence coefficient matrices (Frind, 1982; Therrien and Sudicky, 1996), avoiding the need to numerically integrate the discretized equations that govern fluid flow and heat transfer.

2.2 Governing Equations

2.2.1 Fluid Flow

Variable-density fluid flow in porous media can be described by (Voss, 1984)

$$\frac{\partial}{\partial x_i} \left(\frac{\rho_l \kappa}{\mu} \left\{ \frac{\partial P}{\partial x_j} + \rho_l g \frac{\partial z}{\partial x_j} \right\} \right) = \rho_l S_{op} \frac{\partial P}{\partial t} + \phi \frac{\partial \rho_l}{\partial t} \quad i, j=1,2,3 \quad (1)$$

where ρ_l [$M \cdot L^{-3}$] is water density, κ [L^2] is permeability, μ [$M \cdot L^{-1} \cdot T^{-1}$] is dynamic water viscosity, P [$M \cdot L^{-1} \cdot T^{-2}$] is fluid pressure, g [$L \cdot T^{-2}$] is gravity, ϕ [-] is porosity, and S_{op} [$M^{-1} \cdot L \cdot T^2$] is specific pressure storativity, given by (Voss, 1984)

$$S_{op} = (1 - \phi) \alpha_s + \phi \alpha_l \quad (2)$$

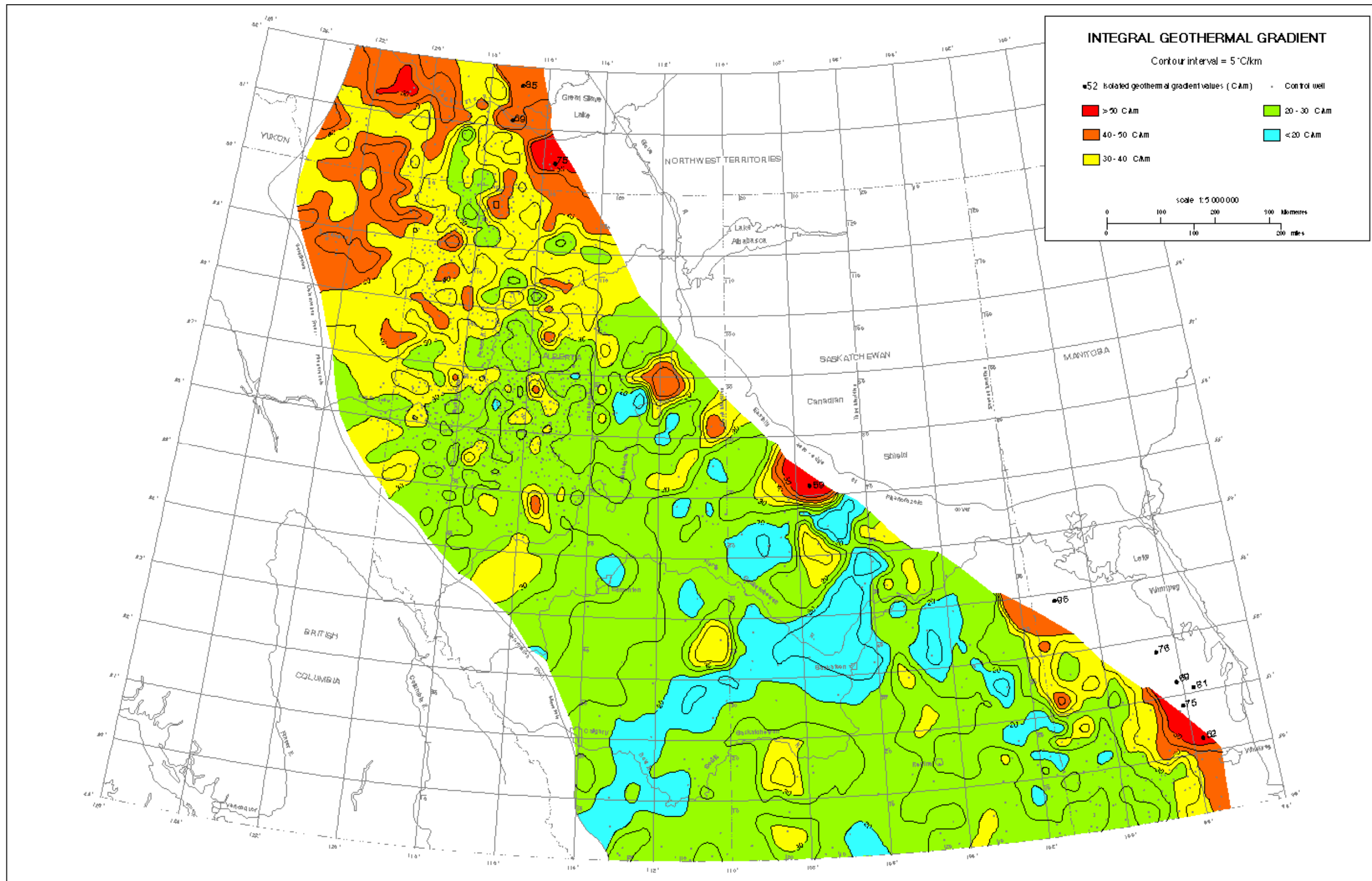


Figure 3. Horizontal distribution of the integral geothermal gradient (between bottom and top of the sedimentary column) in the Western Canada Sedimentary Basin (Bachu and Burwash, 1994).

where α_s [$M^{-1} \cdot L \cdot T^2$] and α_l [$M^{-1} \cdot L \cdot T^2$] are compressibility of the solid and liquid phase, respectively. Equation (1) can be subject to the first-type (Dirichlet) boundary condition

$$P = P_0 \quad (3)$$

or to the second-type (Neumann) boundary condition

$$\frac{\partial P}{\partial n} = \Phi \quad (4)$$

where P_0 [$M \cdot L^{-1} \cdot T^{-2}$] is the imposed constant fluid pressure and Φ [$M \cdot L^{-2} \cdot T^{-2}$] is the imposed constant-fluid-pressure gradient.

2.2.2 Heat Transfer

Under transient flow conditions, heat is transported by convection, conduction, mechanical heat dispersion and radiation. In nature, the temperatures of the solid phase and its contained fluids are different because heat transfer is a transient process. However, both temperatures can be assumed identical because heat transfer between the phases is a fast process relative to other heat-transfer mechanisms (Holzbecher, 1998).

Convection describes heat transfer by movement of a fluid mass. Conductive transport occurs without mass displacement but within the medium due to a temperature gradient alone. Conduction depends, therefore, on the thermodynamic properties of the medium. If groundwater velocity is low, conduction is the dominant heat-transfer mechanism, whereas convection becomes more important in high-velocity environments. Mechanical heat dispersion results from heterogeneity of the medium at all spatial scales, and it is usually neglected in heat-transfer models because it is typically several orders of magnitude smaller than heat conduction. Radiation of heat can be understood as electromagnetic waves and is therefore entirely independent of both the temperature and the thermodynamic properties of the medium. Consequently, the amount of thermal energy transferred through radiation cannot be quantified at a given point in the medium (Planck, 1906) and radiation is therefore commonly ignored in numerical heat-transfer models. The analogous processes of convection, conduction and mechanical heat dispersion for the solute-transport case are advection, molecular diffusion and mechanical dispersion, respectively. The conductive-convective heat-transfer equation in porous media can be written in a form similar to that given by Molson et al. (1992) as

$$\frac{\partial}{\partial x_i} \left(k_b \frac{\partial T}{\partial x_j} - q_i \rho_l \tilde{c}_l T \right) = \rho_b \tilde{c}_b \frac{\partial T}{\partial t} \quad i, j=1,2,3 \quad (5)$$

where k [$M \cdot L \cdot T^{-3} \cdot \Theta^{-1}$] is thermal conductivity, q_i [$L \cdot T^{-1}$] is Darcy flux, ρ [$M \cdot L^{-3}$] is density and \tilde{c} [$L^2 \cdot T^{-2} \cdot \Theta^{-1}$] is specific heat. The temperature in Celsius, T [Θ], is the average temperature between the solid and the liquid phase (Domenico and Schwartz, 1998). The subscripts 'l' and 'b' refer to the liquid and bulk phases, respectively. A gaseous phase is absent. In equation (1), it is also assumed that external heat sinks and sources due to chemical reactions (dissolution/precipitation) are negligible. The heat capacity, $\rho \tilde{c}$ [$M \cdot L^{-1} \cdot T^{-2} \cdot \Theta^{-1}$], denotes the heat removed or gained from a unit volume for a unit change in temperature (Domenico and Schwartz, 1997). Bulk properties $\rho_b \tilde{c}_b$ and k_b can be quantified by considering the volume fractions of the solid and the liquid phase, according to Bolton et al. (1996), as

$$\rho_b \tilde{c}_b = (1 - \phi) \rho_s \tilde{c}_s + \phi \rho_l \tilde{c}_l \quad (6)$$

$$k_b = (1 - \phi)k_s + \phi k_l \quad (7)$$

where the subscript 's' refers to the solid phase. Equation (5) can be subject to the first-type (Dirichlet) boundary condition

$$T = T_0 \quad (8)$$

or to the second type (Neumann) boundary condition

$$\frac{\partial T}{\partial n} = \Gamma \quad (9)$$

where T_0 [Θ] is the imposed constant fluid temperature and Γ [Θ•L⁻¹] is the imposed constant fluid temperature gradient.

2.2.3 Constitutive Equations

Constitutive equations are required to close the system of governing equations (1) and (5). Equations (1) and (5) are physically coupled through the Darcy flux and water-density/viscosity variations. Darcy flux can be calculated as

$$q_i = -\frac{\kappa}{\mu} \left(\frac{\partial P}{\partial x_j} + \rho_l g \frac{\partial z}{\partial x_j} \right) \quad i, j=1,2,3 \quad (10)$$

Water density in kg•m⁻³ is given (Thiesen et al., 1900) as

$$\rho_l = 1000 \cdot \left\{ 1 - \frac{(T - 3.9863)^2}{508929.2} \cdot \frac{T + 288.9414}{T + 68.12963} \right\} \quad (11)$$

Different relations to calculate fluid viscosity from temperature are used to cover different temperature ranges (Molson et al., 1992; Holzbecher, 1998):

$$\mu = \begin{cases} 1.787 \times 10^{-3} \cdot \exp((-0.03288 + 1.962 \times 10^{-4} \cdot T) \cdot T) & \text{for } 0^\circ\text{C} \leq T \leq 40^\circ\text{C} \\ 10^{-3} \cdot (1 + 0.015512 \cdot (T - 20))^{-1.572} & \text{for } 40^\circ\text{C} < T \leq 100^\circ\text{C} \\ 0.2414 \cdot 10^{(247.8/(T + 133.15))} \cdot 10^{-4} & \text{for } 100^\circ\text{C} < T \leq 300^\circ\text{C} \end{cases} \quad (12)$$

where T is in Celsius and μ is in kg•m⁻¹•sec⁻¹. Both water functions are illustrated in Figure 4. Note that the density function respects the water-density maximum at 3.9863°C, and that water viscosity can vary by one order of magnitude within the temperature range of interest.

2.2.4 Coupled System

In nature, the processes of fluid flow and heat transfer are physically coupled because the pressure distribution controls convective geothermal flow and, conversely, the temperature distribution controls water flow through density and viscosity variations. There are two numerical methods that solve coupled problems: 1) the direct-substitution method (DSA), and 2) the sequential-iterative approach (SIA).

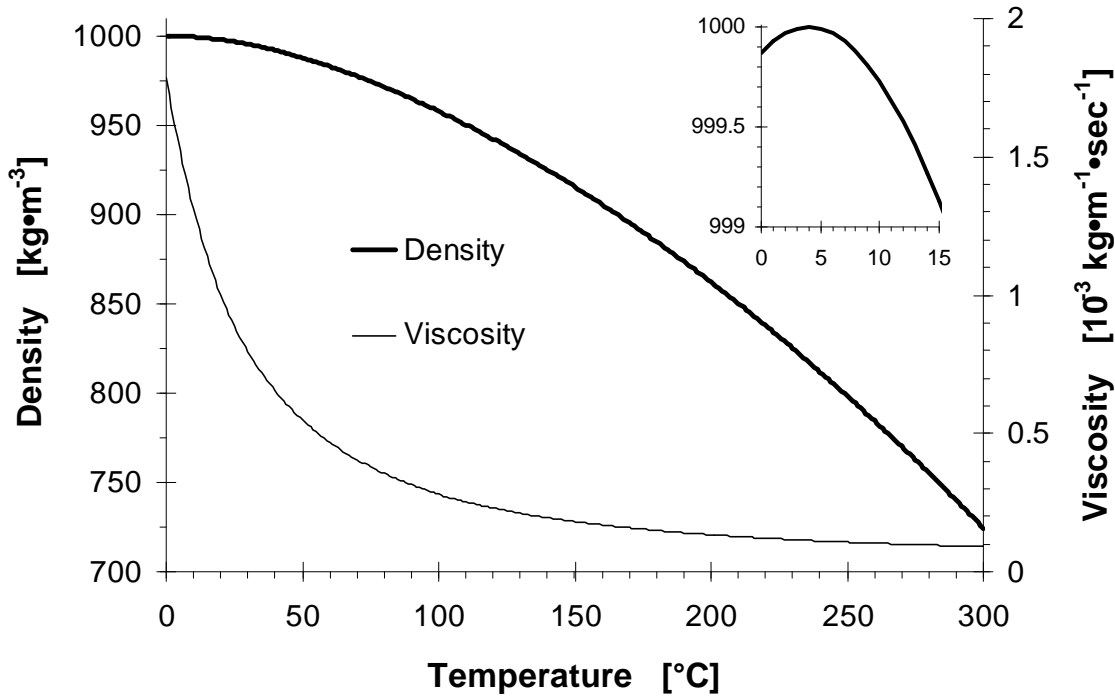


Figure 4. Variation of water density and viscosity with temperature. The inset chart shows the water-density function around the density maximum of 3.9863°C.

In the DSA, the temperature-dependent buoyancy term, $\rho_l g \partial z / \partial x_j$ from equation (1) or (10) is directly substituted in the physical-flow equation, giving a single equation that is finally solved in a single noniterative step (e.g., Ibaraki, 1998). Fluid pressures can be considered as initially unknown. Since iteration is not necessary, the DSA is faster than the SIA. The direct-substitution technique is accurate for a problem with limited density-species (e.g., only temperature) but, for real field problems with multiple density-species (e.g., temperature, sodium and chloride), models built on this approach can suffer from computer-memory limitations.

The SIA is based on the assumption that each density-species can be transported individually in a sequential manner, firstly by density-invariant advective flow and secondly by the impact on fluid density and viscosity. The two steps can then be coupled through an iterative approach. Several models have been developed using the sequential-iterative technique (e.g., Frind, 1982; Voss, 1984; Oldenburg and Pruess, 1998; Shikaze et al., 1998; Frolkovič and De Schepper, 2000; Diersch and Kolditz, 2002; Graf and Therrien, 2005). The advantage of this approach is that resolution of variable-density geothermal flow in two steps (fluid flow and thermal transport) will reduce the number of simultaneous equations to be solved, which is a substantial gain in saving millions or billions of bytes of computer memory.

The HydroGeoSphere model presented here uses the SIA (for variable-density flow problems, also called Picard iteration) to couple fluid flow and geothermal transport. The process flowchart is illustrated in Figure 5.

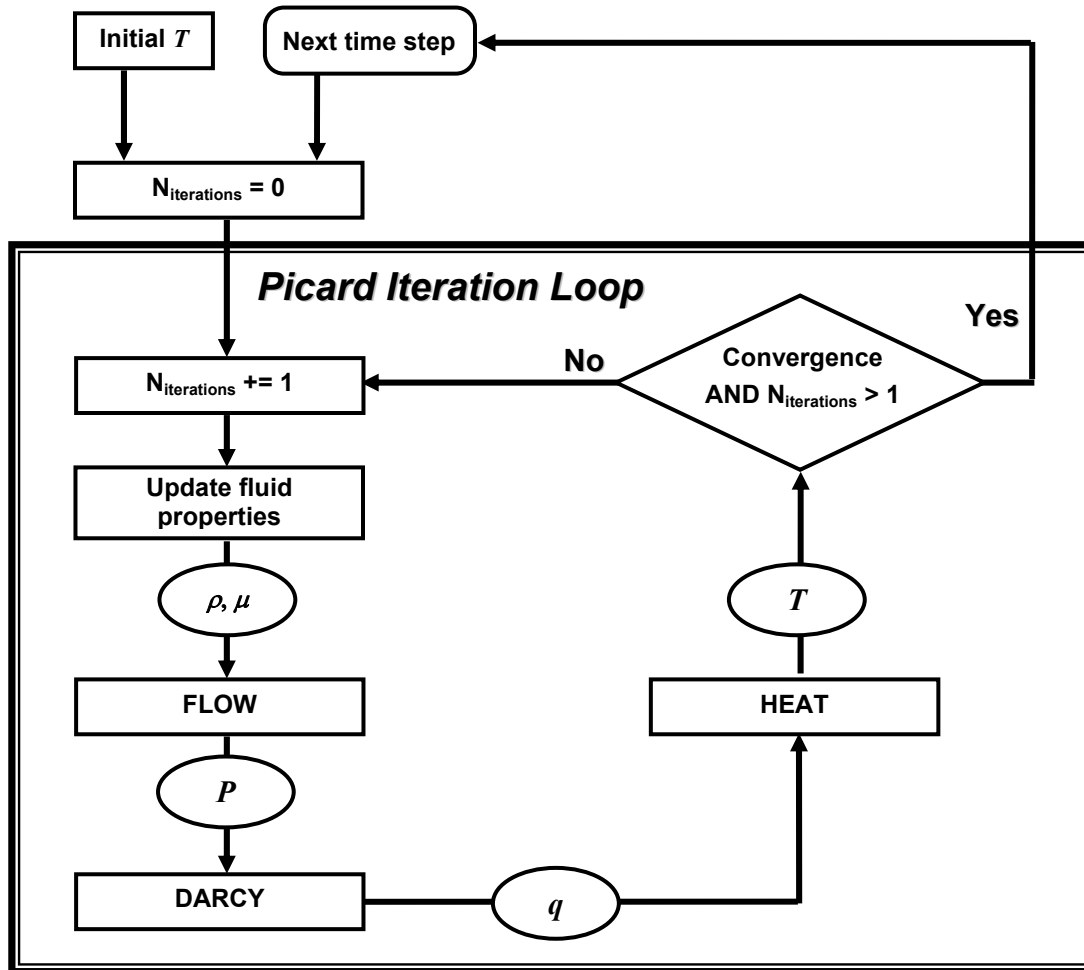


Figure 5. Picard iteration to solve for variable-density variable-viscosity geothermal flow.

2.3 Model Development

The HydroGeoSphere model has been modified to simulate the coupled system shown in Figure 5. The fluid-flow equation (1) is discretized using the control-volume finite-element (CVFE) approach, and the heat-transfer equation (5) is discretized using the Galerkin finite-element approach. Discretizing equations (1) and (5) results in a global-matrix equation of the form

$$\mathbf{A} \cdot \mathbf{u} = \mathbf{b} \quad (13)$$

where \mathbf{A} is the system matrix, \mathbf{u} is the vector of unknowns (pressure or temperature) and \mathbf{b} is a known vector. Equation (13) is finally solved using the WATSIT iterative-solver package for general sparse matrices (Clift et al., 1996) and a conjugate-gradient-stabilized (CGSTAB) acceleration technique (Rausch et al., 2005). A more detailed description of the numerical methods used can be found in Istok (1989).

Convergence of the solution is verified by comparing maximum relative changes of pressure and temperature during a single time-step with a user-defined threshold value. A reasonable choice for the threshold value is 0.1% (e.g., Shikaze et al., 1994). Using a relative-convergence criterion is superior to an absolute-convergence criterion because absolute values of the unknowns can be several orders of

magnitude different. However, a relative-convergence criterion is independent of the absolute value of a variable. The relative-convergence threshold can be defined by the user differently for pressure and temperature. For example, the user may impose maximum changes of 0.5% for pressure and 0.1% for temperature. In addition to the relative-convergence criterion, the Picard iteration loop is only terminated if the number of iterations is larger than one. This second convergence criterion ensures feedback between fluid flow and geothermal transport through at least one iteration.

2.4 Model Verification

The enhanced HydroGeoSphere model has been verified with the Elder (1967) problem of free thermal convection, and with the Caltagirone (1982) analytical solution for the onset of convection using Rayleigh theory.

2.4.1 Elder (1967) Problem

Elder introduced this problem in 1967 to study density-driven thermal convection in porous media due to nonuniform heating of a 2-D domain from below (Figure 6). The 2-D domain is a vertically oriented sand tank filled with a homogeneous isotropic medium. The elevated temperature of 20°C decreases water density, thereby creating a potentially unstable situation where denser fluid overlies less dense fluid. This situation leads to upwelling of warm water and to the formation of thermal fingering. Simulation parameters are listed in Table 1. Given the symmetry of the simulation domain, numerical models typically only consider the half-domain (right or left) to save the cost of computer time. Elder's actual laboratory apparatus was 20 cm long and 5 cm high, but we use a 2-D domain with physical dimensions and parameters scaled for similarity to Elder's work (Voss and Souza, 1987).

The half-domain was spatially discretized using a relatively coarse grid of 60 by 32 elements. Time-step size was held constant at 1 month. The flow and temperature fields at $t = 2$ years are shown in Figure 7.

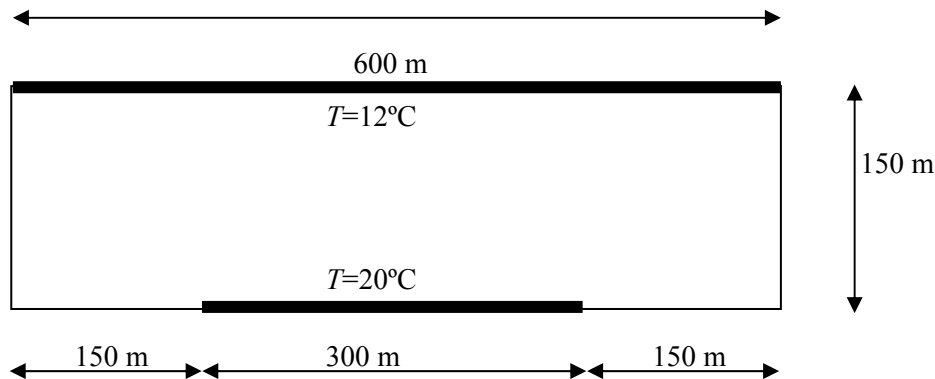


Figure 6. Configuration of the Elder (1967) problem. All boundaries are impermeable to flow.

Table 1. Parameters for the Elder (1967) thermal-convection problem (Oldenburg et al., 1995).

Symbol	Quantity	Value	Unit
ϕ	porosity	0.1	-
κ	permeability	1.21×10^{-10}	m^2
μ	viscosity (T=20°C)	1.0×10^{-3}	$\text{kg} \cdot \text{m}^{-1} \cdot \text{sec}^{-1}$
k_b	thermal conductivity	1.49	$\text{kg} \cdot \text{m} \cdot \text{sec}^{-1} \cdot \text{K}^{-1}$
\tilde{c}_s	heat capacity of rock	0.0	$\text{m}^2 \cdot \text{sec}^{-2} \cdot \text{K}^{-1}$
g	gravity	9.81	$\text{m} \cdot \text{sec}^{-2}$
$T(t=0)$	initial temperature	12.0	°C

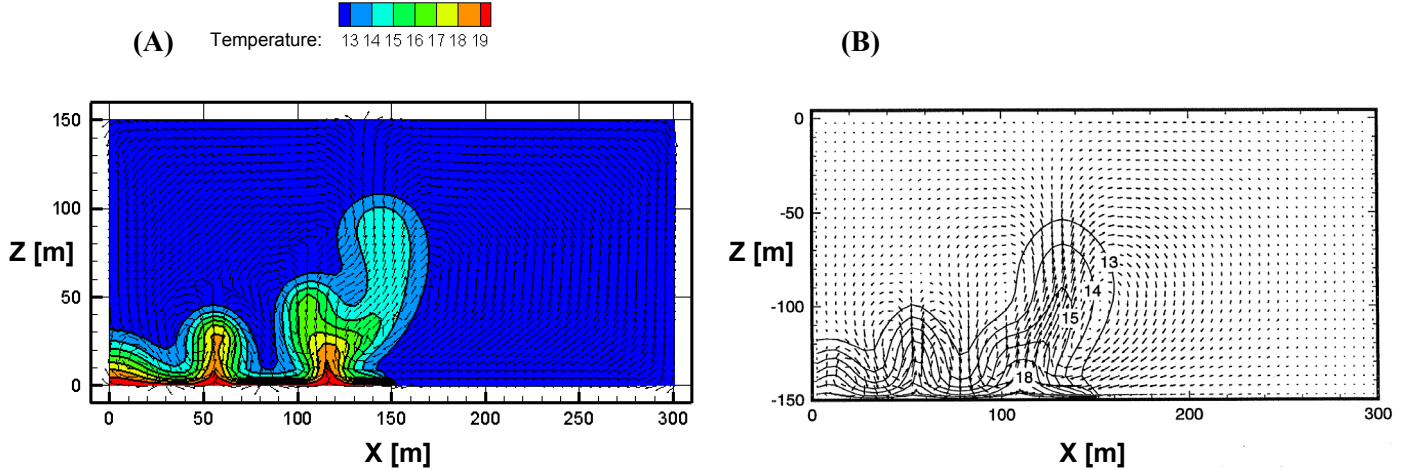


Figure 7. Verification of the HydroGeoSphere model with the Elder (1967) problem of free thermal convection. The figures show isotherms in the half-domain after two years of simulation time from (A) HydroGeoSphere, and (B) TOUGH2 (Oldenburg et al., 1995).

2.4.2 Caltagirone (1982) Analytical Solution

The analytical solution derived by Caltagirone (1982) defines the condition for the onset of free thermal convection in homogeneous isotropic media using a box-type domain of various aspect ratios.

In homogeneous isotropic media, the onset of free geothermal convection can be determined by the value of the dimensionless Rayleigh number, Ra (Rayleigh, 1916). The Rayleigh number is the ratio between buoyancy forces driving free convective flow and conductive forces tending to dissipate unstable flow by enhanced mixing. The thermal Rayleigh number is defined as

$$Ra = \frac{\text{convection}}{\text{conduction}} = \frac{\kappa \cdot g \cdot H \cdot \Delta\rho_l}{\mu \cdot D^{th}} \quad (14)$$

where H [L] is the height of the model domain (in the z -direction) and $\Delta\rho_l$ [$\text{M} \cdot \text{L}^{-3}$] is the fluid-density difference between the top and bottom of the domain. Thermal diffusivity, D^{th} [$\text{L}^2 \cdot \text{T}^{-1}$], is given by

$$D^{th} = \frac{k_b}{\rho_l \tilde{c}_l} \quad (15)$$

If temperature differences are small and/or heat conduction is large, Ra is small, indicating that the system is nonconvecting (conductive regime). On the other hand, a large temperature difference and/or less conduction may cause density-driven flow (convective regime). In this case, the Rayleigh number exceeds the critical Rayleigh number Ra_c , which defines the transition between conductive-only (small Ra) and conductive-convective (large Ra) flow. The value of Ra_c depends on 1) boundary conditions, and 2) aspect ratios.

In an infinitely extended 3-D horizontal layer, the value of Ra_c depends only on the boundary conditions for flow and heat transfer. If all domain boundaries are impermeable to flow, top and bottom boundaries are assigned constant temperatures and all other boundaries are assigned zero-conductive flux conditions, Ra_c has the value $4\pi^2$ (Nield and Bejan, 1999). Square convection cells of width H form in a system where $Ra > 4\pi^2$.

In a 3-D horizontal layer of finite extension, the value of Ra_c also depends on how well convection cells ‘fit’ in the domain. The ability of cells to fit in the domain depends on two aspect ratios, A and B (Horton and Rogers, 1945; Lapwood, 1948)

$$A = \frac{L}{H} \quad B = \frac{W}{H} \quad (16)$$

where L [L] and W [L] are length and width of the box domain, respectively. Caltagirone (1982) accounted for the dependence of Ra_c on aspect ratios. He presented an analytically derived critical Rayleigh number for a 3-D bounded layer

$$Ra_c = \min_{i,j} \left\{ \frac{\pi^2 \cdot \left(\frac{i^2}{A^2} + \frac{j^2}{B^2} + k^2 \right) \cdot \left(A^2 i^2 k^2 + B^2 j^2 k^2 + (i^2 + j^2)^2 \right)}{(i^2 + j^2)^2} \right\} \quad (17)$$

where i, j and k are integers. The 2-D solution to equation (17) is achieved by setting $j = 0$. In this case, the critical Rayleigh number is only a function of aspect ratio A

$$Ra_c = \min_i \left\{ \frac{\pi^2 \cdot \left(\frac{i^2}{A} + k^2 A \right)^2}{i^2} \right\} \quad (18)$$

If and only if the aspect ratio A is an integer, the critical 2-D Rayleigh number Ra_c reaches the minimum value $4\pi^2$. In this case, all convection cells form undistorted perfect circles. If A is not an integer, Ra_c exceeds the minimum value $4\pi^2$ because convection cells cannot form in their preferred circular shape. For $A < 1$, Ra_c can be several orders of magnitude larger than its minimum.

The enhanced HydroGeoSphere model was verified using the Caltagirone (1982) analytical solution for 2-D conductive-convective geothermal flow (equation 18). Figure 8 shows the conceptual model used. A

2-D vertical slice has been chosen where bottom and top are assigned constant temperatures, giving the density difference $\Delta\rho_l$ in equation (14). Water viscosity was held constant at $1.1 \times 10^{-3} \text{ kg}\cdot\text{m}^{-1}\cdot\text{sec}^{-1}$. For different aspect ratios A , the critical Rayleigh number has been calculated with equation (18) and compared with the Rayleigh number calculated with equation (14). Conductive regimes were identified by the absence of a circular velocity field and horizontal undistorted isotherms. A total of 27 simulations with varying aspect ratio and Rayleigh number was carried out. The results were classified as ‘convective’ or ‘conductive’. According to theory, simulations with $Ra < Ra_c$ are conductive, whereas systems with $Ra > Ra_c$ exhibit convective, unstable variable-density flow with varying numbers of rolls. The rare situation of $Ra = Ra_c$ defines a metastable situation (similar to the situation where a seal balances a balloon on its nose) that can change to either ‘convective’ or ‘conductive’. Figure 9, which plots the conductive versus convective flow behaviour, shows that the analytical solution (18) correctly separates conductive from convective regimes.

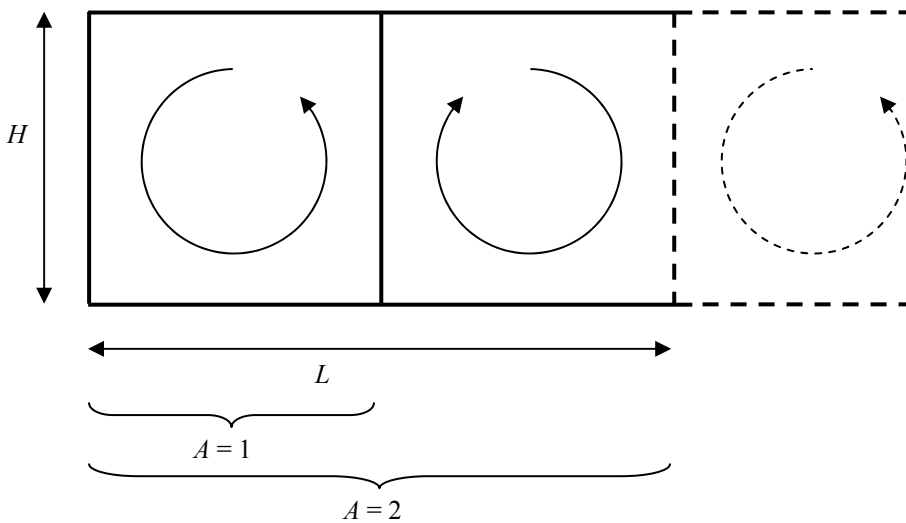


Figure 8. Conceptual 2-D model for the model verification with the Caltagirone (1982) analytical solution.

3 Geothermal Test Case

This section discusses the usefulness of the Elder (1967) problem and the Caltagirone (1982) analytical solution as geothermal test cases, and recommends how to best verify a new geothermal flow model.

Although the Elder (1967) problem represents a natural scenario of free thermal convection in an aquifer system, its usefulness is limited by a number of numerical artifacts:

- **Spatial discretization (coarse vs. fine):** Oldenburg and Pruess (1995) presented the first indication that the Elder problem is highly sensitive to grid discretization. The central heat-transport direction in a coarse grid is upwards (Figure 7), whereas a finer grid exhibits central downwelling. Interestingly, Frolkovič and De Schepper (2000) found that, for an extremely fine grid, a central upwelling characteristic develops again. Frolkovič and De Schepper (2000) have also shown that simulations with a locally adaptive grid are identical to the result using the extremely fine grid.

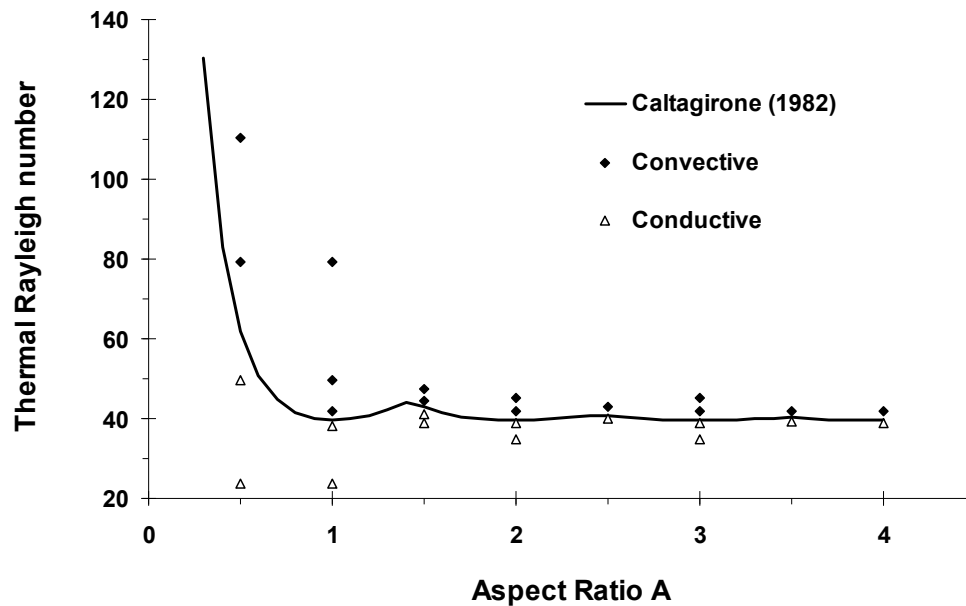


Figure 9. Verification of the HydroGeoSphere model with the Caltagirone (1982) analytical solution.

- Coupling between flow and transport equations (DSA vs. SIA):** Oldenburg and Pruess (1995) used the DSA to couple flow and transport, whereas Voss and Souza (1987) solved the equations in sequence (SIA). It can be shown that the results differ depending on the type of coupling.
- Spatial weighting of advective flux (central vs. upstream):** Frolkovič and De Schepper (2000) discussed the dependency of the Elder result on the type of spatial weighting used for advective flux in the transport equation. When using central weighting of velocities, Frolkovič and De Schepper (2000) found that 1) the result is more prone to the formation of independent thermal energy drops, and 2) temperature values can be negative. Large negative oscillations develop especially for a coarse grid. On the other hand, use of full upstream weighting produces coherent contours without independent drops and does not generate negative temperatures.
- Level of Oberbeck-Boussinesq approximation (level 1 - 2 - 3):** Kolditz et al. (1998) showed that the Elder result depends on the level of the Oberbeck-Boussinesq (OB) approximation applied in the model. The OB assumption reflects to what degree density variations are accounted for (Oberbeck, 1879; Boussinesq, 1903). It is common to consider density effects only in the buoyancy term of the Darcy equation (10) and to neglect density in both flow and heat-transport equations. This first level of the OB assumption is correct if spatial-density variations are minor relative to the value of density (Kolditz et al., 1998). The second level of the OB assumption also accounts for density variations in the flow equation, whereas the third level fully represents density variations in the Darcy equation as well as in both flow and heat-transport equations. In level 3, the continuity equations for fluid and temperature are directly discretized without being simplified. Kolditz et al. (1998) pointed out that level 1 is appropriate when simulating the Elder problem because results from levels 2 and 3 are prone to forming independent temperature drops.

The Caltagirone (1982) analytical solution seems constructed, but it does not suffer from the presence of numerical artifacts. For the Caltagirone (1982) solution, the presence or absence of convection does not depend on the spatial grid or numerical method used by the groundwater software. In addition, simulations can be classified in conductive and convective regimes in an objective manner by inspecting

the velocity field. Therefore, the Caltagirone (1982) solution is not prone to subjective judgement. However, a drawback of the Caltagirone (1982) solution may be the occasionally long simulation time, especially when the Rayleigh number is only slightly smaller or larger than the critical Rayleigh number.

In conclusion, the Elder (1967) problem is a useful geothermal test case if the spatial discretization is identical to that of the compared reference result. However, fully rigorous verification is only achieved by applying the Caltagirone (1982) analytical solution and by creating a plot similar to that shown in Figure 9.

4 Model Applicability and Outlook

The enhanced HydroGeoSphere model is applicable to geothermal reservoirs where the temperature varies between 0° and 300°C. The model fully accounts for density and viscosity variations of formation fluids. The new model has been verified against existing numerical and analytical solutions of variable-density thermal flow in porous media.

The geothermal-energy industry in Alberta is small but growing, and is currently restricted to the use of near-surface, low-grade geothermal heat for heating and cooling purposes in the domestic and small-commercial sectors (Grobe et al., 2009). Although there are considerable temperature data from drill-stem tests and borehole logs, data quality is highly variable, so it is difficult to make accurate predictions of what the temperature will be at a given location and given depth. Consequently, more high-quality information on heat flow and thermal conductivity is needed. In Alberta, many Paleozoic formations in the deeper part of the Alberta basin are potentially suitable for geothermal-energy production (where the assumed minimum temperature is 100°C). Use of the enhanced HydroGeoSphere model presented in this report can provide geological information to identify these formations.

Although water temperature undoubtedly has a major effect on fluid properties, water salinity may also significantly affect fluid density and viscosity. The salinity effect on fluid properties was ignored in this study. In Paleozoic formations suitable for geothermal-energy production, however, water salinities can reach more than 300 000 mg/L total dissolved solids (especially in formations associated with evaporites, such as the Elk Point Group), which is almost ten times that of average seawater. Clearly, the impact of salinity on fluid density and viscosity must be taken into account to characterize geothermal-heat flow in Alberta. Consequently, the impact of the thermal and haline (thermohaline) effects on fluid properties for the prediction of thermohaline flow will be the subject of future numerical studies in Alberta.

5 References

- Bachu, S. (1989): Analysis of heat transfer processes and geothermal pattern in the Alberta Basin, Canada; *Journal of Geophysical Research*, v. 93, p. 7767–7781.
- Bachu, S. and Burwash, R.A. (1994): Geothermal regime in the Western Canada Sedimentary Basin; *in* Geological atlas of the Western Canada Sedimentary Basin, G.D. Mossop and I. Shetsen (comp.), Canadian Society of Petroleum Geologists and Alberta Research Council, Special Report 4, URL <http://www.ags.gov.ab.ca/publications/wcsb_atlas/atlas.html> [February 2009].
- Bolton, E.W., Lasaga, A.C. and Rye, D.M. (1996): A model for the kinetic control of quartz dissolution and precipitation in porous media flow with spatially variable permeability: formulation and examples of thermal convection; *Journal of Geophysical Research*, v. 101, no. B10, p. 22157–22187.
- Boussinesq, V.J. (1903): *Théorie analytique de la chaleur* [Analytical Theory of Heat Transfer]; Gauthier-Villars, Paris, France, v. 2., 362 p.
- Caltagirone, J.P. (1982): Convection in a porous medium; *in* Convective transport and instability phenomena, J. Zierp and H. Oertel (ed.), Braunsche Hofbuchdruckerei und Verlag, Karlsruhe, Germany, p. 199–232.
- Clift, S.S., D'Azevedo, F., Forsyth, P.A. and Knightly, J.R. (1996): WATSIT-1 and WATSIT-B Waterloo sparse iterative matrix solvers; user guide with developer notes for version 2.0.0, 40 p.
- Diersch, H.-J.G. and Kolditz, O. (2002): Variable-density flow and transport in porous media: approaches and challenges; *Advances in Water Resources*, v. 25, no. 8–12, p. 899–944.
- Domenico, P.A. and Schwartz, F.W. (1998): *Physical and chemical hydrogeology*; John Wiley & Sons, New York, 506 p.
- Elder, J.W. (1967): Transient convection in a porous medium; *Journal of Fluid Mechanics*, v. 27, no. 3, p. 609–623.
- Energy Information Administration (1991): *Geothermal energy in the western United States and Hawaii: resources and projected electricity generation supplies*; United States Department of Energy, DOE/EIA-0544, URL <<http://www.eia.doe.gov/cneaf/solar.renewables/renewable.energy.annual/backgrnd/fig19.htm>> [June 2009].
- Frind, E.O. (1982): Simulation of long-term transient density-dependent transport in groundwater; *Advances in Water Resources*, v. 5, no. 2, p. 73–88.
- Frolkovič, P. and De Schepper, H. (2000): Numerical modeling of convection dominated transport coupled with density driven flow in porous media; *Advances in Water Resources*, v. 24, no. 10, p. 63–72.
- Graf, T. and Therrien, R. (2005): Variable-density groundwater flow and solute transport in porous media containing nonuniform discrete fractures; *Advances in Water Resources*, v. 28, no. 12, p. 1351–1367.
- Grobe, M., Richardson, R.J.H., Johnston, K., Quibell, J., Schillereff, H.S. and Tsang, B. (2009): Importance of geoscience information in the implementation of closed-loop, ground-source heat-pump systems (geoexchange) in Alberta; Energy Resources Conservation Board, ERCB/AGS Open File Report 2009-09, 49 p.
- Hitchon, B. (1969): Fluid flow in the Western Canada Sedimentary Basin, 1. Effect of topography; *Water Resources Research*, v. 5, no. 1, p. 186–195.

- Hitchon, B. (1984): Geothermal gradients, hydrodynamics, and hydrocarbon occurrences, Alberta, Canada; AAPG Bulletin, v. 68, no. 6, no. 713–743.
- Holzbecher, E.O. (1998): Modeling density-driven flow in porous media; Springer Verlag, Berlin, Germany, 286 p.
- Horton, C.W. and Rogers, F.T., Jr. (1945): Convective currents in a porous medium; Journal of Applied Physics, v. 16, p. 367–370.
- Ibaraki, M. (1998): A robust and efficient numerical model for analyses of density-dependent flow in porous media; Journal of Contaminant Hydrology, v. 34, no. 10, p. 235–246.
- Istok, J. (1989): Groundwater modeling by the finite element method; American Geophysical Union, Washington, DC, 495 p.
- Kolditz, O., Ratke, R. Diersch, H.-J.G. and Zielke, W. (1998): Coupled groundwater flow and transport: 1. Verification of variable-density flow and transport models; Advances in Water Resources, v. 21, no. 1, p. 27–46.
- Lam, H.L. and Jones, F.W. (1986): An investigation of the potential for geothermal energy recovery in the Calgary area in southern Alberta, Canada, using petroleum exploration data; Geophysics, v. 51, no. 8, DOI:10.1190/1.1442215.
- Lapwood, E.R. (1948): Convection of a fluid in a porous medium; Proceedings of the Cambridge Philosophical Society, v. 48, p. 508–521.
- Majorowicz, J.A. and Jessop, A.M. (1981): Regional heat flow patterns in the Western Canadian Sedimentary Basin; Tectonophysics, v. 74, p. 209–238.
- Molson, J.W.H., Frind, E.O. and Palmer, C. (1992): Thermal energy storage in an unconfined aquifer 2. Model development, validation and application; Water Resources Research, v. 28, no. 10, p. 2857–2867.
- Nield, D.A. and Bejan, A. (1999): Convection in porous media; Springer Verlag, New York, 546 p.
- Oberbeck, A. (1879): Ueber die Wärmeleitung der Flüssigkeiten bei Berücksichtigung der Strömung infolge von Temperaturdifferenzen [On the thermal conductivity of flowing liquids in a temperature field]; Annalen der Physik und Chemie, v. 7, p. 271–292.
- Oldenburg, C.M., Hinkins, R.L., Moridis G.J. and Pruess, K. (1995): On the development of MP-TOUGH2; Proceedings of TOUGH Workshop 1995, Lawrence Berkeley Laboratory, Berkeley, California.
- Oldenburg, C.M. and Pruess, K. (1995): Dispersive transport dynamics in a strongly coupled groundwater-brine flow system; Water Resources Research, v. 31, no. 2, p. 289–302.
- Oldenburg, C.M. and Pruess, K. (1998): Layered thermohaline convection in hypersaline geothermal systems; Transport in Porous Media, v. 33, p. 29–63.
- Planck, M. (1906): Vorlesungen über die Theorie der Wärmestrahlungen [Lectures on the theory of heat radiation]; Verlag von Johann Ambrosius Barth, Leipzig, Germany, 222 p.
- Rausch, R., Schäfer, W., Therrien, R. and Wagner, C. (2005): Solute transport modelling: an introduction to models and solution strategies; Borntraeger, Stuttgart, Baden-Württemberg, Germany, 205 p.
- Rayleigh, J.W.S. (1916): On convection currents in a horizontal layer of fluid when the higher temperature is on the under side; Philosophical Magazine Series 6, v. 32, no. 192, p. 529–546.
- Shikaze, S.G., Sudicky, E.A. and Mendoza, C.A. (1994): Simulations of dense vapour migration in discretely-fractured geologic media; Water Resources Research, v. 30, no. 7, p. 1993–2009.

- Shikaze, S.G., Sudicky, E.A. and Schwartz, F.W. (1998): Density-dependent solute transport in discretely-fractured geologic media: is prediction possible?; *Journal of Contaminant Hydrology*, v. 34, no. 10, p. 273–291.
- Therrien, R. and Sudicky, E.A. (1996): Three-dimensional analysis of variably saturated flow and solute transport in discretely-fractured porous media; *Journal of Contaminant Hydrology*, v. 23, no. 6, p. 1–44.
- Therrien, R., McLaren, R.G., Sudicky, E.A. and Panday, S.M. (2008): Hydrogeosphere—a three-dimensional numerical model describing fully integrated subsurface and surface flow and solute transport; Université Laval and University of Waterloo, Canada (free PDF available from senior author).
- Thiesen, M., Scheel, K. and Diesselhorst, H. (1900): Untersuchungen über die thermische Ausdehnung von festen und tropfbar flüssigen Körpern – Bestimmung der Ausdehnung des Wassers für die zwischen 0° und 40° liegenden Temperaturen [Investigation of the thermal expansion of solid and liquid materials – Determination of the expansion of water between 0°C and 40°C]; *Wissenschaftliche Abhandlungen der Physikalisch-Technischen Reichsanstalt*, v. 3, p. 1–70.
- Voss, C.I. (1984): SUTRA: a finite-element simulation model for saturated-unsaturated fluid density-dependent groundwater flow with energy transport or chemically reactive single-species solute transport; United States Geological Survey, Water Resources Investigation Report 84-4369, 409 p.
- Voss, C.I. and Souza, W.R. (1987): Variable density flow and solute transport simulation of regional aquifers containing a narrow freshwater-saltwater transition zone; *Water Resources Research*, v. 23, no. 10, p. 1851–1866.